RSC Advances

PAPER

View Article Online
View Journal | View Issue

Cite this: *RSC Adv.*, 2021, **11**, 20760

Blue nanocomposites coated with an ionic liquid polymer for electrophoretic displays

Yue Hu,[a] Salah Ahmed Sarhan Al-Shujaa,[a] Bin Zhen,[c] Yaping Zhang,[ab]* Xianggao Li[a] and Yaqing Feng*[a]

Received 6th April 2021
Accepted 23rd May 2021

DOI: 10.1039/d1ra02683f

rsc.li/rsc-advances

Electrophoretic display (EPD) is a type of flexible display which has attracted wide attention. In this work, blue nanosized crystals of cobalt aluminum oxide ($CoAl_2O_4$) were precipitated on silica nanoparticles, and then the nanocomposites were coated with an ionic liquid polymer (PIL) to give blue electrophoretic particles. The blue nanocomposites (SCAs) formed possess an excellent spherical structure, and the average diameter is about 188 nm. The porous silica matrix presents a relative light density, and the blue $CoAl_2O_4$ pigment offers excellent color. The outside ionic liquid polymer supplies the PIL/SCAs with a light density of 1.7915 g cm^{-3}, excellent hydrophobicity and dispersion stability in the electrophoretic liquid. The fabricated single-particle EPD prototypes show a response time of 165 ms in the EPD cell with a 0.2 mm thickness, which is much faster than the commercial EPDs, and this is probably because of the unique composite structure.

Introduction

Flexible displays have become one of the hot research topics, because of their mechanical flexibility, high scalability, low weight and large-area production compatibility. The electrophoretic display (EPD) is one type of flexible display which attracts much attention due to its unique properties including a paper-like appearance, ultralow power consumption and good flexibility.[1,2]

Electrophoretic particles are the key component of the electrophoretic display, and their color and electrophoretic property have a remarkable affect on the display properties. At present, organic pigments are usually used to color the electrophoretic particles.[3–5] Organic pigments provide almost all types of color series and have a suitable low density for electrophoretic systems. However, decomposition of organic pigments in organic electrophoretic liquid often leads to a short service lifetime of EPDs.

Inorganic pigments usually possess excellent optical, electrical and chemical properties and have a long service lifetime.[6,7] However, the finite existing color series and large density limit their application in EPDs. The large density of the inorganic pigment makes it very easy to sediment out in the suspension fluid. Use of electrophoretic particles with a hollow structure have been proposed to decrease the density,[8,9] but their poor mechanical strength cannot be neglected. An inorganic pigment coated with polymer is another option for reducing its apparent density, which in addition favors the improvement of the dispersion stability.[10–12] At the moment, polymers are mostly coated onto the surface of particles through weak physical interaction, which leads to a swelling problem and affects their lifetime badly. Meanwhile, general polymer coatings always offer poor surface charge performance and show a low responding speed in electric fields.[13]

In this work, blue inorganic nanocrystals are precipitated on the surface of silica nanospheres to obtain blue inorganic pigments. Next, the inorganic pigments are modified by a silane coupling agent, which further reacts with the ionic liquid monomer to achieve electrophoretic particles coated with ionic liquid polymers. The porous silica nanoparticles have a relatively low density, excellent mechanical strength, and rich surface hydroxyl groups for reacting with the silane coupling agent. The ionic liquid polymer coating would offer light density, good dispersion stability and suitable electrophoretic property.

Experimental

Materials and reagents

Triton X-100, *n*-hexane, and tetraethoxysilane (TEOS) were purchased from Shanghai Titan Scientific. Triethoxyvinylsilane, *n*-hexanol, *n*-dodecyl bromide, 1-vinylimidazole, methylamine solution, divinylbenzene and potassium persulfate were obtained from the Aladdin Industrial Corporation. All reagents were analytically pure grade and used as-received.

Preparation of blue inorganic nanoparticles

Two methods were investigated for preparing the blue inorganic nanoparticles. The first one was a post-modification method.

[a]*School of Chemical Engineering and Technology, Tianjin University, Tianjin 300072, China. E-mail: zhypin126@126.com; yqfeng@tju.edu.cn*

[b]*School of Materials and Environment, Beijing Institute of Technology, Zhuhai, Zhuhai 519085, China*

[c]*College of Chemistry and Chemical Engineering, Tianjin University of Technology, Tianjin 300384, China*

Firstly, white silica nanoparticles were prepared according to a process reported previously.[14] Next, 1.0865 g of urea (or ammonia with the same molar dosage) was added into an aqueous solution containing 0.3291 g of $Co(NO_3)_3 \cdot 6H_2O$, 0.8483 g of $Al(NO_3)_3 \cdot 9H_2O$ and 21.73 g of water. After the reaction at 95 °C for 30 min, 1.00 g of the white silica nanoparticles were added into the solution. The reaction was kept at 95 °C for 120 min to form grey-blue colored particles. The grey-blue particles were washed three times with ethanol and dried at 60 °C for 180 min under vacuum. Finally, the blue inorganic nanoparticles were obtained after calcination at 1000 °C for 120 min and denoted as SCAs-1.

Another method was an *in situ* method using a sol–gel process and reverse microemulsion. Firstly, *n*-hexane (35.80 g), *n*-hexanol (19.62 g), Triton X-100 (30.00 g) and methylamine aqueous solution (20 wt%, 3 mL) were mixed together under vigorous stirring to give a reverse microemulsion solution. Then, an *n*-hexane solution of TEOS (10 wt%, 30 mL) was added dropwise. As the TEOS moved from the oil-phase into the water-core of the reverse micelles, the sol–gel process started. After reacting at 35 °C for 60 min, an aqueous solution containing 0.3291 g of $Co(NO_3)_3 \cdot 6H_2O$ and 0.8483 g of $Al(NO_3)_3 \cdot 9H_2O$ was added into the reaction system. The $CoAl_2O_4$ precursors formed and were deposited on the surface of the silica particles as the reaction proceeded. Lastly, the composite precursors were collected and calcined at 1000 °C for 120 min to give the blue $CoAl_2O_4/SiO_2$ nanoparticles (SCAs-2).

Preparation of the blue PIL/SCAs nanoparticles

Triethoxyvinylsilane (0.84 g) and 1.00 g of SCAs-2 were added into 10 mL of deionized water, and reacted at 100 °C for 24 h. After washing with acetone, followed by drying, the modified blue particles were obtained and denoted as VSCAs.

The [VDoIm][Br] ionic liquid was synthesized by a previously reported method.[14] The [VDoIm][Br] (0.64 mmol), 0.2 g of VSCAs and 0.32 mmol of divinylbenzene were added into deionized water, and the reaction was initiated with 0.16 mmol $K_2S_2O_8$ at 70 °C. After reacting for 180 min, the nanoparticles were washed with acetone, and then dried to give blue PIL/SCAs nanoparticles.

Characterization

The SEM images were obtained using a S-4800 (Hitachi) field emission microscope. The FTIR spectra were collected on a Nicolet 380 (Thermo Electron) infrared spectroscope. Particle size dispersity and zeta potential analysis were carried out using a Delsa™ Nano C (Beckman Coulter) particle size and zeta potential analyzer. The zeta value and mobility value of the samples in the electrophoretic liquids were collected directly using a high concentration test attachment. The TGA was carried out on a SDT Q500 (TA Instruments). The XRD was conducted on an Ultima IV X-ray diffractometer (Rigaku, Japan). The N_2 physisorption measurement was carried out on an Autosorb iQ2 MP (Quantachrome Instruments, USA), and the powdered samples were outgassed in a 9 mm cell at 200 °C for 3 h before the measurements were made. The X-ray photoelectron spectroscopy (XPS) was carried out on a RBD upgraded PHI-5000C ESCA system (PerkinElmer) with Mg Kα radiation ($h\frac{1}{4}$ = 1253.6 eV). The contact angle of the samples before and after surface modification was conducted on a JC2000D contact angle goniometer (Powereach) with a manual drop dispenser, image capture system and a manual high-precision three-dimensional platform. The samples were pressed into pieces, and water was used as the test solvent. The CIE chromaticity diagrams were measured using an X-Rite Eye-One Pro colorimeter (North LCD Engineering R&D Center, China). The response time of the fabricated EPD prototype was determined on an electrophoretic particle device property analyzer (North LCD Engineering R&D Center, China).

Fabrication of EPD prototype

Two pieces of ITO-coated glass substrates were arranged in parallel-plate capacitor geometry with the conducting surfaces face-to-face, and a polyurethane film was sandwiched between them to form a cell of 10 × 20 × 0.2 mm. The electrophoretic liquid, a dispersion of sample particles in tetrachloroethylene with the addition of CH-5 additive, was injected into the cell to observe the display performance under the electric field intensity of 20 V μm^{-1}.

Results and discussion

Formation of blue silica nanoparticles

In the proposed structure of the SCAs, the porous silica nanoparticles acted as the matrix, and the $CoAl_2O_4$ endowed the nanoparticles with the blue color.

The first idea was to coat the blue $CoAl_2O_4$ nanocrystals onto silica nanoparticles by post-coprecipitation. The silica nanoparticles were prepared previously, and then the Co^{2+} and Al^{3+} ions were coprecipitated onto the surface of the silica nanoparticles with the assistance of alkalis, such as ammonia and urea. As shown in Fig. 1(a), the prepared silica nanoparticles possess a monodisperse spherical structure. After the coprecipitation, SEM of the obtained SCAs was performed and the resulting images are shown in Fig. 1(b) and (c), and it can be seen that the silica nanoparticles have been corroded. Even at low concentrations, both ammonia and urea would damage the structure of the silica spheres.

In previous work, the formation of the silica nanoparticles in a reverse microemulsion has been studied in detail.[14] The monodisperse silica sols and gels formed successively in the polar microreactors dispersed in a nonpolar solvent, with assistance of alkali. Coprecipitation of Al^{3+} ions and Co^{2+} ions on silica nanoparticles was also performed under alkaline conditions. Immediately, coupling of the sol–gel process of silica precursors with the coprecipitation of Al^{3+} ions and Co^{2+} ions was proposed. Therefore, Co^{2+} and Al^{3+} ions were directly added into the reaction system during the formation of silica sols. Unfortunately, it was found in that the products obtained were tiny particles with an average diameter of 20–50 nm (Fig. 1(d)), which was obviously much less than that of the silica nanoparticles. This occurred because the addition of electrolytes (Co^{2+} and Al^{3+} ions) destroyed the framework of the silica sols, and the silica nanospheres broke into tiny particles.[15,16]

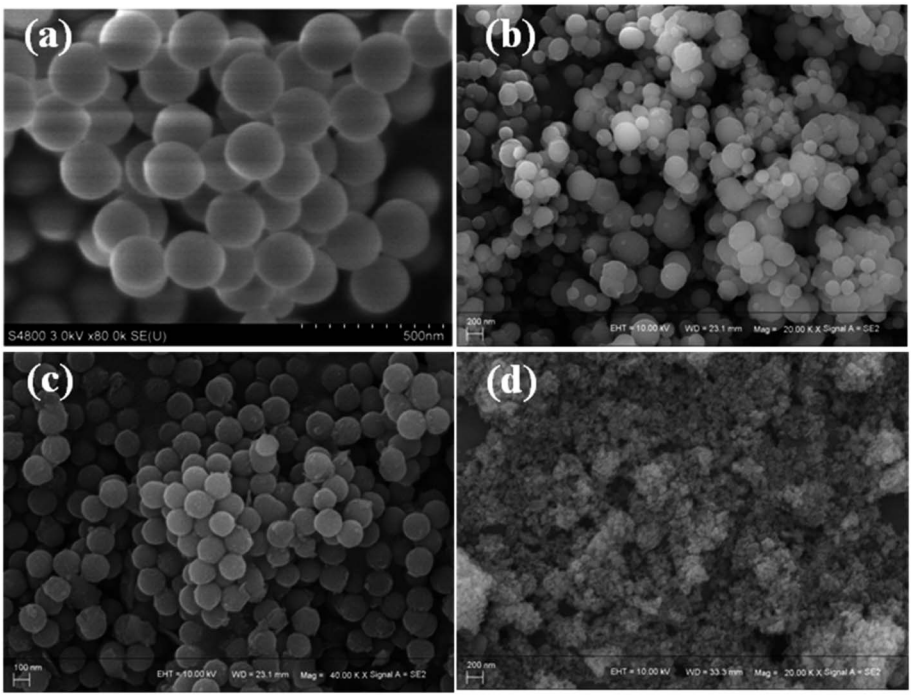

Fig. 1 The SEM images of silica nanoparticles (a), the SCAs-1 post-coprecipitated with ammonia (b) and urea (c), and the samples obtained by direct coupling of the silica sols with ions (d).

In order to introduce the $CoAl_2O_4$ nanocrystals into the silica nanoparticles, the most effective time to add the Al^{3+} ions and the Co^{2+} ions into the system should be considered. To have the best chance of combining silica spheres with the pigment $CoAl_2O_4$, the detailed formation process of the matrix silica nanoparticles was studied. It was found that during the formation process, silica nanoparticles with a stable structure could form when the reaction in the micelles lasted for at least 60 min. If the metal ions were added into the reaction system after this time, then it was more likely that the reaction would

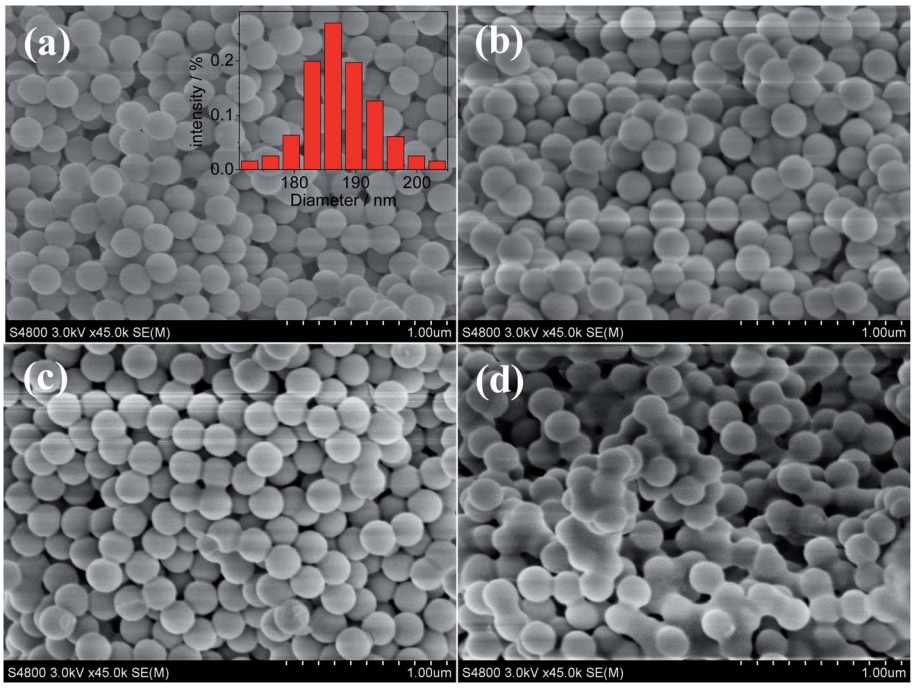

Fig. 2 The SEM images of the samples during the formation of SCAs-2. (a) 30 min, (b) 45 min, (c) 60 min, and (d) 90 min. The inset in (a) is statistical particle size distribution of the SCAs-2.

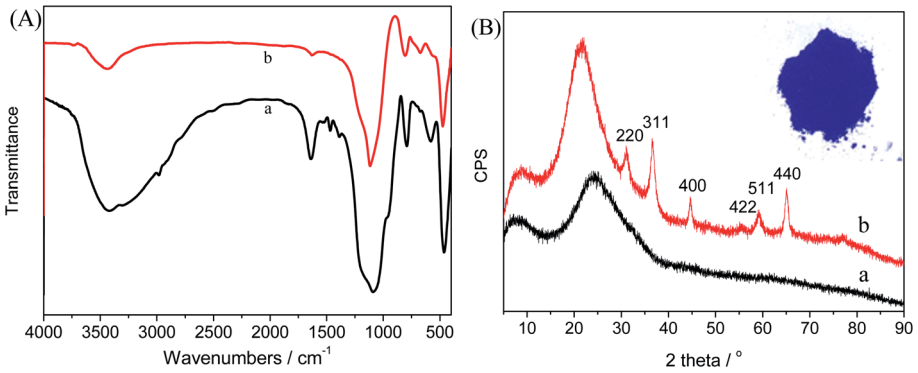

Fig. 3 (A) The FTIR spectra of the composite precursors (a), and SCAs-2 (b). (B) The XRD patterns of the composite precursors (a), and SCAs-2 (b), and the inset is a photograph of the SCAs-2.

work. Hence, a reverse microemulsion containing a Co^{2+} and Al^{3+} aqueous solution was added into the system after the initial reaction had progressed for 75 min. After the addition of the reverse microemulsion containing Co^{2+} and Al^{3+} ions, the reaction system was sampled as the reaction time proceeded. After washing and calcination, the blue particles were collected. The SEM images of the samples are shown in Fig. 2. It can be observed that when the coprecipitation goes on for 30 min, the particles formed possess a spherical structure, and the average diameter is about 188 nm (the inset shown in Fig. 2(a)). As the reaction time continues, the average diameter of the particles showed no obvious change, whereas a sintering problem happened between the particles. This was probably because the further hydrolysis of the silica sols and ions caused the formation of the bonds between the particles.

Structure and properties of blue nanoparticles

The chemical composition and structure of the SCAs-2 were investigated using FTIR, XRD, TEM and XPS analyses.

The FTIR spectra and XRD patterns of the inorganic composite precursors and SCAs-2 are shown in Fig. 3. As shown in Fig. 3(A), after calcination, the characteristic peaks, such as 2983 cm^{-1} and 2935 cm^{-1}, 1520 cm^{-1}, 1468 cm^{-1}, 1388 cm^{-1}, disappear, and the characteristic peaks of free water and hydroxyl at 3550–3300 cm^{-1} and 1635 cm^{-1}, respectively, decrease remarkably. At the same time, the amorphous inorganic composite became crystalline. The XRD pattern of the SCAs-2 is shown in Fig. 3(B). The diffraction peaks at 36.52°, 31.02°, 44.62°, 59.22°, and 65.10° were assigned to the lattice planes of 311, 220, 400, 511 and 440, respectively. This illustrated the formation of the spinel $CoAl_2O_4$ phase.

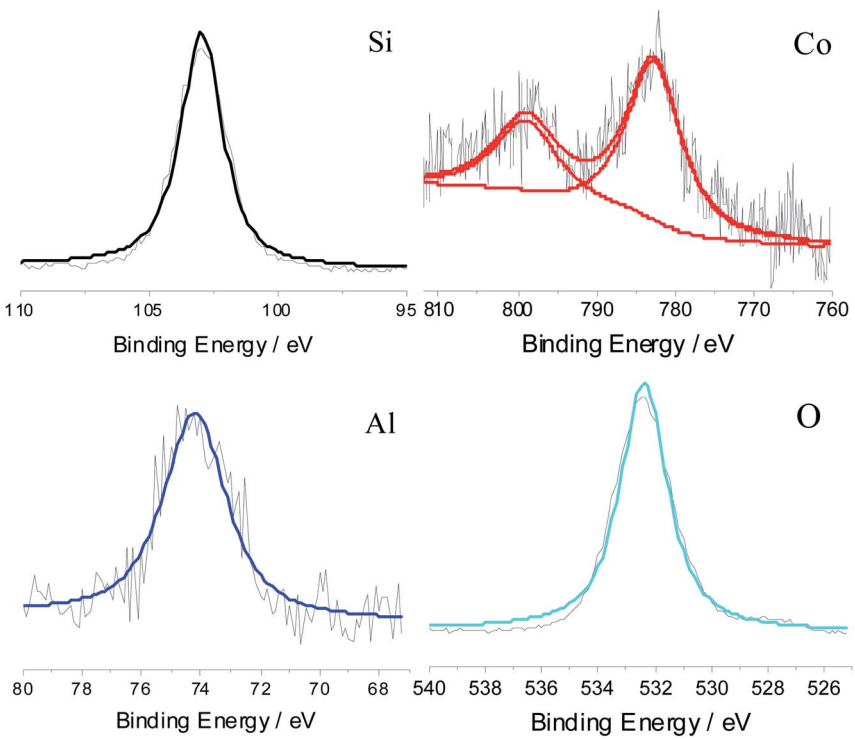

Fig. 4 The XPS curves obtained for the SCAs-2.

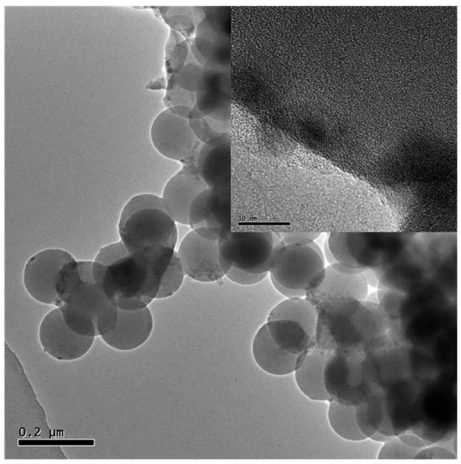

Fig. 5 A TEM image of SCAs-2. The inset is a magnified image.

The element analysis was carried out using XPS, and aluminum, cobalt, oxygen and silicon, elements were all found, as shown in Fig. 4. The silicon element came from silica, and the cobalt and aluminum have valences of +2 and +3, respectively. This proves that silica and aluminum cobalt oxide were formed. In addition, the atomic percent of silicon (2p), aluminum (2p) and cobalt (2p) were 21.5%, 1.4% and 1.0%, respectively. This proves that the mass ratio of $CoAl_2O_4$ to silica was equal to 11%, which was close to the set value.

The TEM images of the SCAs-2 are shown in Fig. 5. This also proved that the SCAs-2 had a spherical shape. In the magnified image (inset of Fig. 5), it was also seen that tiny spinel $CoAl_2O_4$ particles gathered on the surface of the SCAs-2, giving them a bright blue color. The density of the samples was determined using the density bottle method. For the $CoAl_2O_4$ particles prepared under the same reaction conditions, its density was 6.2354 g cm^{-3}. Compared with $CoAl_2O_4$, the density of SCAs-2 was reduced dramatically to 2.3414 g cm^{-3}. This proved that the existence of the silica matrix dramatically decreased the density of the SCAs-2.

As the preparation process has shown, as the surface modification proceeds, some of the hydroxyl groups on the surface of the SCAs-2 reacted with triethoxyvinylsilane, and the following anchored vinyl groups polymerized with the vinyl groups of the ionic liquids, until the PIL/SCAs were generated. When compared with the FTIR spectrum of the SCAs-2 (Fig. 3(A)), the FTIR spectrum of the modified SCAs-2 shown in Fig. 6(A) shows some characteristic peaks of [VDoIm][Br]. The peaks at 1630 cm^{-1}, 1606 cm^{-1}, and 1448 cm^{-1}, 1412 cm^{-1} were assigned to the stretching vibration of imidazole ring and benzene ring, respectively, and 3065 cm^{-1} and 3024 cm^{-1} were assigned to the unsaturated C–H bond. The peaks at 2925 cm^{-1} and 2854 cm^{-1} were assigned to the saturated C–H bond, and 2959 cm^{-1} was assigned to the methylene group.

After surface modification, the density of the prepared VCSAS and PIL/SCAs was reduced further to 1.9668 g cm^{-3} and 1.7915 g cm^{-3}, respectively. This was because of the introduction of organic components. The dispersion stability of the electrophoretic particles in dispersant largely depended on the density of the electrophoretic particles.[17,18] According to the density value of the PIL/SCAs, its deviation from the solvent density was smaller than 0.5 g cm^{-3}, which means that the density of the prepared nanoparticles is close to that of the solvent and is therefore suitable for use as an electrophoretic liquid. In addition, the surface modification showed an evident influence on the surface property of the SCAs-2. As shown in Table 1, the wetting angle value of the PIL/SCAs was much bigger than that of the SCAs-2, which indicated that the VSCAs showed a lower hydrophilicity. For the SCAs-2, the plentiful hydroxyl groups on the surface helped them to easily disperse in water because of the formation of hydrogen bonds. By comparison, after surface modification, some of hydroxyl groups were consumed, and the ionic liquid polymers were introduced. The long alkyl groups of the ionic liquid polymers covered the surface of the particles. All these factors result in the much higher hydrophobicity of the PIL/SCAs. Furthermore, the long alkyl groups of the ionic liquids could also help to mitigate the agglomeration of PIL/SCAs dispersed in the hydrophobic electrophoretic liquid.

The morphology of the prepared VSCAs and PIL/SCAs were also observed using SEM, and the images obtained, showing the spherical structure of the particles, are displayed in Fig. 7. The TEM images (Fig. 8) proved the spherical structure and the existence of the organic ionic liquid polymer which coats the particle surface, and the thickness of the ionic liquid polymer on the surface of PIL/SCAs was about several nanometers. In

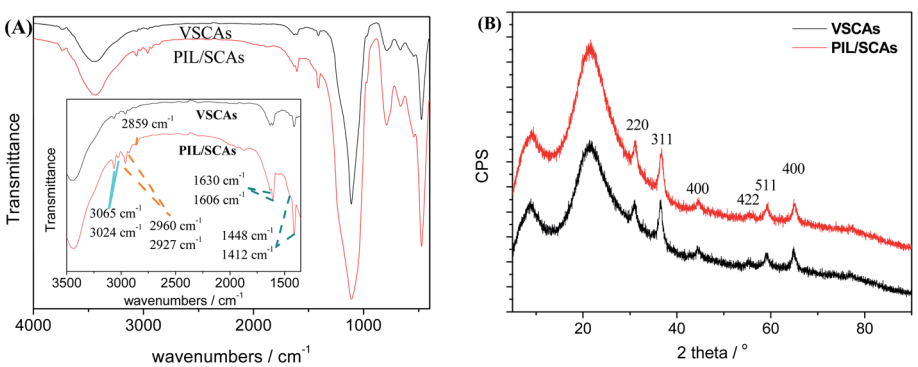

Fig. 6 The FTIR spectra (A), and XRD patterns (B) of VSCAs and PIL/SCAs.

Table 1 The properties of silica nanoparticles at various reaction times

Sample	Density/g cm^{-3}	Pore volume/g cm^{-3}	Pore diameter $D_v(d)$/nm	Surface area[a]/m^2 g^{-1}	Wetting angle/°
SCAs-2	2.3414	0.321	63.543	22.373	7.7
VSCAs	1.9668	0.261	64.435	21.539	85.47
PIL/SCAs	1.7915	0.233	61.016	19.473	94.68

[a] Calculated by BET.

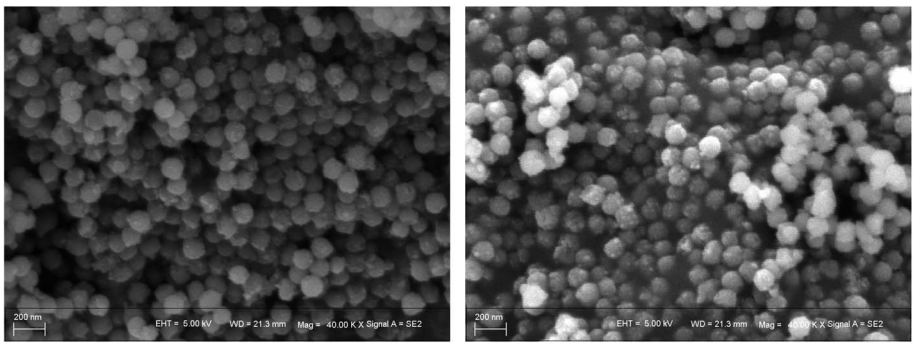

Fig. 7 The SEM images of VSCAs (left) and PIL/SCAs (right).

addition, the XRD patterns of the VSCAS and PIL/SCAs showed that the surface modification of SCAs would not affect the crystal structure of the $CoAl_2O_4$, as shown in Fig. 6(B). It was also found that the blue color of the SCAs did not change during the surface modification.

In order to explore the structure of the PIL/SCAs, the N_2 physisorption isotherms of the samples were then carried out. The N_2 adsorption–desorption isotherms of the samples (Fig. 9(A)) were type III hysteresis curves with a wide pore size distribution (Fig. 9(B)). The lack of isotherm plateauing from $P/P_0 = 0.95$ to 1.0 in the samples was because there was a combination of large mesopores, macropores (pores > 50 nm), and interparticle voids.[19] The pore volume and specific surface area of the silica nanoparticles prepared in a closed system reported previously were 0.415 cm^3 g^{-1} and 22.745 m^2 g^{-1}, respectively, whereas the calculated pore volume and specific surface area of the SCAs-2 were 0.321 cm^3 and 22.373 m^2 g^{-1}. Compared with the silica nanoparticles prepared in the similar system reported previously,[14] the SCAs-2 had a similar pore structure and negligible reduction of pore volume and specific surface area. It was concluded that the introduction of $CoAl_2O_4$ did not affect the mesoporous structure of the silica matrix. After surface modification, the N_2 adsorption–desorption isotherms of the samples did not obviously change, whereas the pore volume and specific surface area of VSCAs and PIL/SCAs shrank gradually. This was because the modified layers occupied part of the pore wall and the surface of the silica matrix. This had the effect that the silica matrix and the surface modification greatly reduced the density of the SCAs-2, and made the particles suitable for use in electrophoretic fluids.

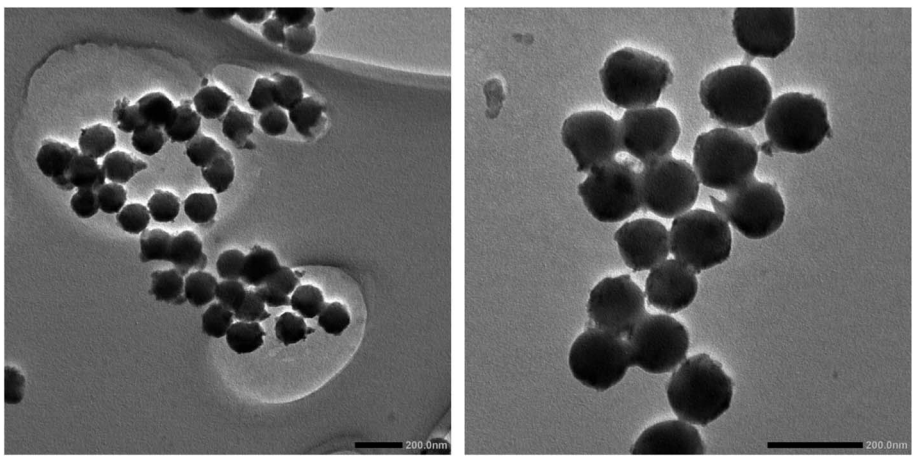

Fig. 8 The TEM images of VSCAs (left) and PIL/SCAs (right).

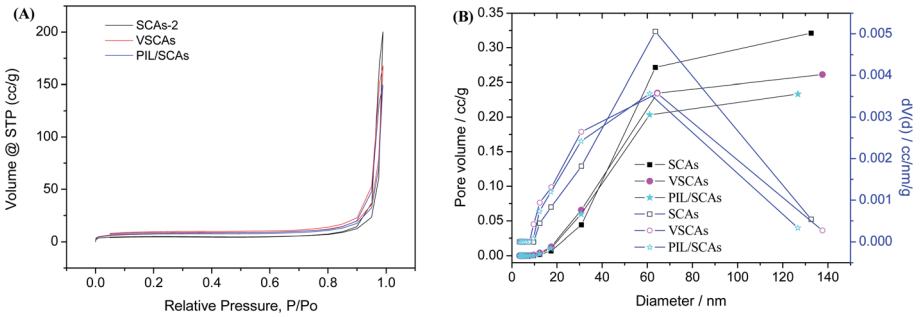

Fig. 9 The N_2 adsorption–desorption isotherms (A), and the pore size distribution curves (B) of the silica nanoparticles.

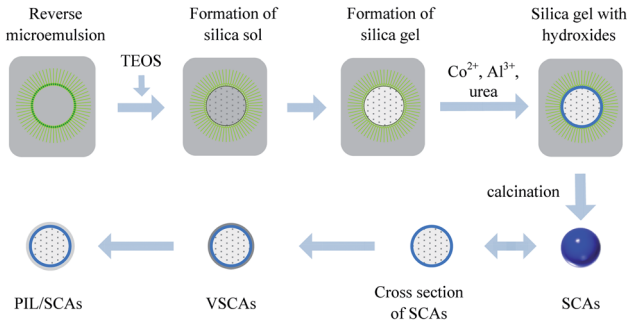

Scheme 1 Schematic diagram showing the proposed preparation method for the PIL/SCAs.

Formation process of PIL/SCAs

Based on the results of the previous analyses, the formation scheme of the SCAs-2 was proposed and is shown in Scheme 1. Firstly, the TEOS dispersed in the reverse microemulsion changed into silica sols with the help of an alkali. Secondly, the crosslinking degree of the silica sols increased and the silica gels formed with the increase of time. Thirdly, the reverse microemulsion containing Al^{3+} and Co^{2+} was added into the reaction system, and the aluminum hydroxides and cobalt hydroxides were precipitated onto the surface of silica gels with the help of the alkali. Fourthly, the blue inorganic pigment SCAs-2 composites formed after calcination. Fifthly, the SCAs-2 were modified with vinyl groups and the VSCAs formed. Finally, the surface polymerization occurred with the addition of [VDoIm][Br], and the PIL/SCAs formed. The PIL/SCAs could be successfully prepared *via* a sol–gel process in reverse microemulsion combined with surface polymerization. The reverse microemulsion provided the samples with a monodisperse and spherical structure, and the silica matrix also helped to decrease the density. The $CoAl_2O_4$ composites gave the sample an excellent blue color, and the ionic liquid polymer coatings gave the prepared particles a low density and hydrophobicity, which was good for the dispersion of the particles in the nonpolar solvent. Thus, the prepared PIL/SCAs are a promising candidate for use as electrophoretic particles.

Electrophoretic property

The coordinates in CIE 1931 chromaticity diagram of the SCAs-2 before and after surface modification are listed in Table 2. The CIE coordinates of the SCAs-2 were (0.2142, 0.1831), and its luminance Y value is 46.41. The chromaticity of the SCAs-2 was close to the blue color of the RGB color model. After surface modification, the hue value changed a little and the luminance value decreased a little. This was probably caused by the shrinking of the surface reflectivity of the organic coating, vinyl modifier and the ionic liquid polymer layers. Based on the previous analysis, both the SCAs-2 and PIL/SCAs showed excellent chromaticity which was suitable for use in EPDs.

In this research, the prepared PIL/SCAs were employed as blue particles to fabricate a single particle prototype EPD. In the fabricated prototype EPD, it was obvious to see that the blue electrophoretic particles swam in the cell and showed blue images. The surface zeta potentials and mobility values of the SCAs-2 and PIL/SCAs in the electrophoretic liquids were determined and are shown in Table 2. Compared with SCAs, the surface zeta and mobility value of PIL/SCAs were obviously improved, and these probably benefited from the ionic liquid polymer on the surface. In the fabricated prototypes with a thickness of 0.2 mm, the response time of the PIL/SCAs is 167 ms. For the modified titania particles reported previously[20,21] and commercial EPDs with a close response distance, the response times were all greater than 260 ms, which was much

Table 2 Chromaticity and mobility of samples[a]

Sample	Y	x	y	Zeta potential/mV	Mobility/cm^2 V^{-1} s^{-1}	Response time/ms
SCAs-2	46.41	0.2142	0.1831	0.32	4.98×10^{-8}	—
VSCAs	46.36	0.2234	0.1947	—	—	—
PIL/SCAs	45.77	0.2251	0.1977	4.13	6.17×10^{-7}	165

[a] The display properties of the EPDs were evaluated under an electric field of 20 V μm^{-1}.

longer than that of the PIL/SCAs. It was probably that the low density and ionic liquid polymer coating of the PIL/SCAs which endowed them the excellent property. The low density decreased their gravitational sedimentation and favored their mobility. The ionic liquid polymer coating not only favored the hydrophobicity and dispersity stability, but also helped to enrich the trace polar impurities around the particles, such as water.[22,23] The polar impurities favored the ionization effect and aided the mobility. With the assistance of electric field, the response time of the prototype EPDs were tested and the results are shown in Table 2. As demonstrated in Table 2, the response property of the applied electric field of the prepared PIL/SCAs was faster than that of the commercial EPDs and the SCAs-2, and this was probably because of the special ionic liquid chains on the surface.[14]

At the same time, TiO_2 nanoparticles were used as the opposite white particles and a blue-white dual-particle prototype EPD was fabricated. A clear white image and a blue image could be displayed, but the response time became longer and the quality of the blue image became lighter. This was probably due to the more complicated interactions between the particles and the hiding power of PIL/SCAs.

Conclusions

In this work, blue $CoAl_2O_4/SiO_2$ nanoparticles (SCAs-2) are prepared by the coupling of a coprecipitation of Co^{2+} and Al^{3+} ions and a sol–gel process in a reverse microemulsion, and then the SCAs-2 are surface-modified and coated with an ionic liquid polymer (PIL/SCAs) by surface solution polymerization. It is found that the moment where the Co^{2+} and Al^{3+} ions are introduced into the reverse microemulsion affects the particle structure badly. During the reaction process, silica nanoparticles with a stable structure could form when the sol–gel reaction in the micelles has proceeded for 60 min, and this was when the Co^{2+} and Al^{3+} ions are added. After reacting for another 30 min, the SCAs-2 are obtained. The prepared SCAs-2 possess a spherical structure, and the average diameter is about 188 nm. The porous silica matrix gives a relatively low density, and the blue $CoAl_2O_4$ pigment gives excellent color. After surface modification, the density of the prepared PIL/SCAs reduced further to 1.7915 g cm^{-3}, its deviation from the solvent density is smaller than 0.5 g cm^{-3}, meaning that the density of the prepared PIL/SCAs is close to the solvent and suitable for use in the electrophoretic liquid. In addition, the PIL/SCAs have excellent hydrophobicity. The long alkyl groups of the ionic liquids could also help to mitigate the agglomeration of PIL/SCAs dispersed in the hydrophobic electrophoretic liquid. The fabricated single-particle EPD prototypes show a response time of 165 ms in the electrophoretic display cell with a thickness of 0.2 mm, which is much faster than that of the commercial EPDs. This probably benefits from the special composite structure. For the EPDs, a chromatic display is urgently needed, and the blue color is one of the important primary colors. In future work, the use of green and red electrophoretic particles still needs more research time, and the micro-encapsulated EPDs also need more attention.

Conflicts of interest

There are no conflicts to declare.

Acknowledgements

This work was financially supported by the National Natural Science Foundation of China (Grant No. 21706185) and the Natural Science Foundation of Tianjin (Grant No. 18JCQNJC06900).

References

1 Y. Chen, J. Au, P. Kazlas, *et al.*, Electronic paper: flexible active-matrix electronic ink display, *Nature*, 2003, **423**, 136.
2 B. Peng, Y. Li, J. Li, *et al.*, Monodisperse light color nanoparticle ink toward chromatic electrophoretic displays, *Nanoscale*, 2016, **8**, 10917–10921.
3 P. P. Yin, G. Wu, W. L. Qin, *et al.*, CYM and RGB colored electronic inks based on silica-coated organic pigments for full-color electrophoretic displays, *J. Mater. Chem. C*, 2013, **1**(4), 843–849.
4 J. J. Han, W. H. Zhang, X. G. Li, *et al.*, Encapsulation of modified copper phthalocyanine (CuPc) via miniemulsion polymerisation for electrophoretic display, *Mater. Res. Innovations*, 2015, **19**(1), 24–27.
5 G. X. Li, S. X. Meng and Y. Q. Feng, Encapsulation of modified pigment yellow 110 (PY110) for electrophoretic display, *J. Mater. Res.*, 2016, **31**(15), 2261–2267.
6 L. S. Park, W. P. Jin, H. Y. Choi, *et al.*, Fabrication of charged particles for electrophoretic display, *Curr. Appl. Phys.*, 2006, **6**, 644–648.
7 Z. Liu, X. Li and S. Wang, Preparation of TiO_2 Nano-particles with Controllable Surface Charges for Electrophoretic Display, *J. Inorg. Mater.*, 2012, **27**, 649–654.
8 S. Wang, Y. Mei, X. Li, *et al.*, Preparation of high efficiency hollow TiO_2 nanospheres for electrophoretic displays, *Mater. Lett.*, 2012, **74**, 1–4.
9 Y. Fang, S. Wang, Y. Xiao, *et al.*, Preparation and properties of red inorganic hollow nanospheres for electrophoretic display, *Appl. Surf. Sci.*, 2014, **317**, 319–324.
10 X. Fang, H. Yang, G. Wu, *et al.*, Preparation and characterization of low density polystyrene/TiO_2 core-shell particles for electronic paper application, *Curr. Appl. Phys.*, 2009, **9**, 755–759.
11 L. Zhang, Y. Jiang, X. Li, *et al.*, Preparation of titanium dioxide nanoparticles modified with methacrylate and their electrophoretic properties, *J. Mater. Sci.: Mater. Electron.*, 2015, **26**, 1–7.
12 G. Li, S. Meng and Y. Feng, Encapsulation of modified pigment yellow 110 (PY110) for electrophoretic display, *J. Mater. Res.*, 2016, **31**, 2261–2267.
13 B. J. Park, S. Y. Hong, H. H. Sim, *et al.*, Effect of charge control agent on electrophoretic characteristics of polymer encapsulated titania nanoparticles, *Mater. Chem. Phys.*, 2012, **135**, 259–263.

14 Y. P. Zhang, B. Zhen, S. Al-Shuja'a, *et al.*, Fast-response and monodisperse silica nanoparticles modified with ionic liquid towards electrophoretic displays, *Dyes Pigm.*, 2018, **148**, 270–275.

15 Y. P. Zhang, B. Zhen, Y. Hu, *et al.*, Reverse micellar system with Triton X-100: effect of surfactant polydispersity and preparation of monodisperse silica nanoparticles, *Soft Matter*, 2020, **16**, 383–389.

16 Y. P. Zhang, H. S. Li, B. Zhen, *et al.*, Study on preparation and properties of mesoporous magnetic silica, *Adv. Mater. Res.*, 2011, **197–198**, 269–272.

17 J. H. Park, A. L. Mi, B. J. Park, *et al.*, Preparation and electrophoretic response of poly(methyl methacrylate – co -methacrylic acid) coated TiO_2 nanoparticles for electronic paper application, *Curr. Appl. Phys.*, 2007, **7**(4), 349–351.

18 S. Liu, J. Yu and M. Jaroniec, Tunable photocatalytic selectivity of hollow TiO_2 microspheres composed of anatase polyhedra with exposed {001} facets, *J. Am. Chem. Soc.*, 2010, **132**(34), 11914–11916.

19 S. M. Egger, K. R. Hurley, A. Datt, *et al.*, Ultraporous mesostructured silica nanoparticles, *Chem. Mater.*, 2015, **27**, 3193–3196.

20 L. Zhang, Y. Jiang, X. Li, S. Wang and Y. Xiao, Preparation of titanium dioxide nanoparticles modified with methacrylate and their electrophoretic properties, *J. Mater. Sci.: Mater. Electron.*, 2015, **26**, 1–7.

21 G. Li, S. Meng and Y. Feng, Encapsulation of modified pigment yellow 110 (PY110) for electrophoretic display, *J. Mater. Res.*, 2016, **31**, 2261–2267.

22 Y. Zhang, Q. Jiao, B. Zhen, Q. Wu and H. Li, Transesterification of glycerol trioleate catalyzed by basic ionic liquids immobilized on magnetic nanoparticles: influence of pore diffusion effect, *Appl. Catal., A*, 2013, **453**, 327–333.

23 B. Zhen, Q. Jiao, Q. Wu, H. Li and Y. Zhang, Acidic ionic liquid immobilized on magnetic mesoporous silica: preparation and catalytic performance in esterification, *Appl. Catal., A*, 2012, **445–445**, 239–245.